

## LETTER

# Sparse-optimized nested L-shaped arrays with hybrid LASSO-PSCM framework for enhanced DOA estimation in mutual coupling environments

Weichuang Yu <sup>1, 2</sup>, Hui Wang<sup>1, a)</sup>, Huiheng Liu<sup>1</sup>, and Gang Li<sup>1</sup>

**Abstract** This paper proposes three novel sparse-optimized nested L-shaped array (LA) configurations (ISNA-LA, ANCADI-S-LA, AINA-LA) to address the challenges of limited degrees of freedom (DOFs) and mutual coupling in conventional LAs. These configurations optimize element placement in two-level nested arrays (TLNAs) to enhance DOFs and reduce mutual coupling via sparse spatial distribution. A hybrid 2-D DOA estimation framework integrating the least absolute shrinkage and selection operator (LASSO) and the pair-matching method by signal covariance matrices (PSCM) is established, enabling full utilization of difference coarray DOFs and automatic azimuth-elevation pairing. Numerical simulations show that the proposed arrays outperform conventional LAs in DOFs and mutual coupling reduction, while the LASSO-PSCM algorithm achieves superior 2-D estimation accuracy.

**Keywords:** direction of arrival (DOA) estimation, L-shaped arrays (LAs), degrees of freedom (DOFs), mutual coupling effect

**Classification:** Antennas and propagation

## 1. Introduction

Direction of arrival (DOA) estimation is pivotal in modern antenna array systems, enabling critical applications in radar, navigation, and wireless communications [1]. While one-dimensional (1-D) arrays face angular resolution limitations, practical scenarios increasingly demand precise two-dimensional (2-D) parameter estimation, driving innovations in array configurations and algorithms.

Among 2-D configurations, L-shaped arrays (LAs) stand out because they feature a simple structure and facilitate extension into various planar array configurations with closed-form expressions. Compared to cross arrays and other simple structured 2-D arrays, LAs achieve superior 2-D DOA estimation accuracy, making them ideal for high-precision applications. Early LA-based methods, such as least squares (LS), maximum likelihood (ML), and multiple signal classification (MUSIC) [2], faced computational complexity and subarray configuration constraints. Subsequent advancements focused on sparse subarrays to enhance degrees of freedom (DOFs) and robustness. For instance, coprime LAs improved source capacity, while nested LAs expanded un-

derdetermined estimation capabilities. Matrix reconstruction techniques and spatiotemporal fusion further advanced angular resolution and noise resilience.

A critical challenge in dense LAs is mutual coupling, which degrades coarray reconstruction. Recent solutions include enlarged element spacing with rotational invariance techniques (ESPRIT) techniques and difference-sum coarray theory [3] to suppress coupling while enlarging DOFs. Despite progress, 2-D DOA estimation remains limited by insufficient DOFs and coupling effects, particularly when decomposing tasks into 1-D subarray estimations. Pair-matching methods like covariance-based PSCM improved angle alignment but struggle with coarray discontinuity in sparse configurations.

To address these limitations, we propose three enhanced LAs (ISNA-LA, ANCADI-S-LA, AINA-LA) based on advanced nested subarrays [4, 5, 6], achieving higher DOFs and reduced mutual coupling. For coarray discontinuity in ANCADI-S-LA and AINA-LA, we develop a hybrid LASSO-PSCM algorithm combining sparse signal reconstruction via least absolute shrinkage and selection operator (LASSO) with the pair-matching method by signal covariance matrices (PSCM). This framework enables full utilization of difference coarray DOFs and automatic azimuth-elevation pairing without computational overhead.

## 2. Signal model with L-shaped array (LA) structure

The traditional LA consists of two orthogonally arranged uniform linear subarrays, with its structure diagram illustrated in Fig. 1. Subarray 1 and subarray 2 comprise  $M$  elements at coordinates  $\mathbb{S}_x$  and  $N$  elements at coordinates  $\mathbb{S}_z$ , respectively. Define the element locations as

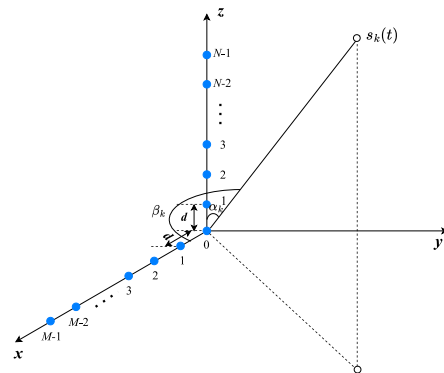


Fig. 1 Structure diagram of conventional LA configuration.

<sup>1</sup> School of Physics and Electronic Engineering, Hubei University of Arts and Science, Xiangyang 441053, China

<sup>2</sup> Guangxi Key Laboratory of Brain-inspired Computing and Intelligent Chips, Guangxi Normal University, Guilin 541004, China

a) tryo@163.com

DOI: 10.23919/comex.2025XBL0063

Received April 15, 2025

Accepted May 29, 2025

Publicized July 11, 2025

Copyedited January 1, 2026



$$\mathbb{S}_x = \{x_m \mid x_m = md, m \in \{0, 1, \dots, M-1\}\} \quad (1)$$

$$\mathbb{S}_z = \{z_n \mid z_n = nd, n \in \{0, 1, \dots, N-1\}\} \quad (2)$$

where  $d = \lambda/2$  denotes the unit inter-element spacing with incident wavelength  $\lambda$ .

Consider  $K$  incoherent far-field narrowband sources impinging on the LA, where the  $k$ -th source  $s_k$  has 2-D DOA parameters  $(\alpha_k, \beta_k)$ , where  $k \in [1, K]$ ,  $\alpha_k \in [0, 180^\circ]$  and  $\beta_k \in [0, 90^\circ]$  represent the azimuth and pitch angles respectively. The 2-D DOA estimation for LAs is typically decomposed into the independent estimation of azimuth angles  $\{\alpha_k\}_1^K$  and elevation angles  $\{\beta_k\}_1^K$  using subarray measurements. The steering vectors  $\mathbf{a}_1(\alpha_k)$  and  $\mathbf{a}_2(\beta_k)$  can be expressed as

$$\mathbf{a}_1(\alpha_k) = \left[1, e^{j2\pi x_1(\cos \alpha_k)/\lambda}, \dots, e^{j2\pi x_{M-1}(\cos \alpha_k)/\lambda}\right]^T \quad (3)$$

$$\mathbf{a}_2(\beta_k) = \left[1, e^{j2\pi z_1(\cos \beta_k)/\lambda}, \dots, e^{j2\pi z_{N-1}(\cos \beta_k)/\lambda}\right]^T \quad (4)$$

where  $\{x_m\}_1^{M-1}$  and  $\{z_n\}_1^{N-1}$  represent the element locations on the  $x$ -axis and  $z$ -axis, respectively.

In the presence of mutual coupling, the received signal model for subarray 1 and subarray 2 at time  $t$  can be expressed as

$$\mathbf{x}_1(t) = \sum_{k=1}^K \mathbf{C} \mathbf{a}_1(\alpha_k) s_k(t) + \mathbf{n}_1(t) = \mathbf{C} \mathbf{A}_1(\alpha) \mathbf{s}(t) + \mathbf{n}_1(t) \quad (5)$$

$$\mathbf{x}_2(t) = \sum_{k=1}^K \mathbf{C} \mathbf{a}_2(\beta_k) s_k(t) + \mathbf{n}_2(t) = \mathbf{C} \mathbf{A}_2(\beta) \mathbf{s}(t) + \mathbf{n}_2(t) \quad (6)$$

where  $\mathbf{s}(t) = [s_1(t), s_2(t), \dots, s_K(t)]^T$  is the source vector whose corresponding power set is  $\{\sigma_1^2, \sigma_2^2, \dots, \sigma_K^2\}$ .  $\mathbf{C}$  is the mutual coupling matrix.  $\mathbf{n}_1(t)$  and  $\mathbf{n}_2(t)$  are independent and identically distributed additive white Gaussian noises,  $\sigma_n^2$  is the noise power.  $\mathbf{A}_1(\alpha)$  and  $\mathbf{A}_2(\beta)$  are array manifold matrices of subarray 1 and subarray 2, given by

$$\mathbf{A}_1(\alpha) = [\mathbf{a}_1(\alpha_1), \mathbf{a}_1(\alpha_2), \dots, \mathbf{a}_1(\alpha_K)] \quad (7)$$

$$\mathbf{A}_2(\beta) = [\mathbf{a}_2(\beta_1), \mathbf{a}_2(\beta_2), \dots, \mathbf{a}_2(\beta_K)] \quad (8)$$

### 3. Proposed method

In this section, we present three sparse-optimized nested L-shaped array configurations and develops a novel 2-D DOA estimation framework integrating LASSO with PSCM.

#### 3.1 Improved nested L-shaped array configurations

Though the traditional two-level nested array LA (TLNA-LA) enlarge DOFs compared to conventional LAs, their subarrays maintain dense element spacing that exacerbates mutual coupling. To address these limitations, we propose three improved configurations (ISNA-LA, ANCADI-S-LA and AINA-LA) through subarray optimization.

For an  $N$ -element subarray with optimized sparse spacing, the element locations set along each axis defined as:

$$\mathbb{S} = \{n_i \mid i = 1, 2, \dots, 2N-1\} \quad (9)$$

Figure 2 illustrates the subarrays and their difference coarrays of four nested LAs with 8 elements. It can be seen that

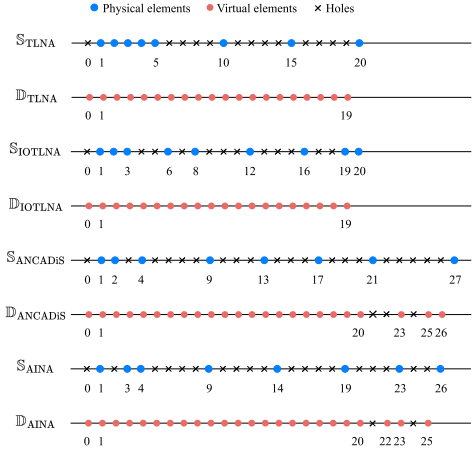


Fig. 2 Structure diagram of conventional LA configuration.

the IOTLNA and TLNA achieve identical DOFs and generate uniform continuous virtual array elements in their difference coarrays. However, IOTLNA experiences lower mutual coupling effects than TLNA due to its fewer compact array elements. Meanwhile, ANCADI-S and AINA configurations attain higher DOFs with reduced mutual coupling, but their difference coarrays contain discontinuities (“holes”). To fully leverage these available DOFs for DOA estimation, compressed sensing (CS) algorithms can be employed.

#### 3.2 LASSO-PSCM method

2-D DOA estimation of nested LAs can be decomposed into two 1-D estimation processes. For configurations with discontinuous difference coarrays (e.g., ANCADI-S/AINA-LAs), the LASSO algorithm is used to overcome the limitations caused by holes in the coarray. The azimuth and elevation angles are subsequently paired using PSCM. This hybrid framework is named LASSO-PSCM.

The 1-D DOA estimate  $\{\hat{\alpha}_k\}_1^K$  for subarray 1 is obtained through the LASSO algorithm. Based on  $\{\hat{\alpha}_k\}_1^K$ , the array manifold matrix of subarray 1 can be derived as follows:

$$\hat{\mathbf{A}}_1 = [\mathbf{a}_1(\hat{\alpha}_1), \mathbf{a}_1(\hat{\alpha}_2), \dots, \mathbf{a}_1(\hat{\alpha}_K)] \quad (10)$$

The following optimization function is constructed to solve the estimated value  $\hat{\mathbf{s}}(t)$  of the source vector  $\mathbf{s}(t)$ :

$$\hat{\mathbf{s}}(t) = \arg \min_{\mathbf{s}(t)} \sum_{t=1}^J \|\mathbf{x}_1(t) - \hat{\mathbf{A}}_1 \mathbf{s}(t)\|_2 \quad (11)$$

Solving Eq. (11) yields

$$\hat{\mathbf{s}}(t) = (\hat{\mathbf{A}}_1^H \hat{\mathbf{A}}_1)^{-1} \hat{\mathbf{A}}_1^H \mathbf{x}_1(t) = \hat{\mathbf{A}}_1^+ \mathbf{x}_1(t) \quad (12)$$

Then the covariance matrix of  $\hat{\mathbf{s}}(t)$  can be obtained

$$\hat{\mathbf{R}}_s = E \{\hat{\mathbf{s}}(t) \hat{\mathbf{s}}^H(t)\} = \hat{\mathbf{A}}_1^+ \mathbf{R}_{11} \hat{\mathbf{A}}_1^H \quad (13)$$

where  $\mathbf{R}_{11}$  is the covariance matrix of the received signal  $\mathbf{x}_1(t)$ , and its expression is

$$\mathbf{R}_{11} = E \{\mathbf{x}_1(t) \mathbf{x}_1^H(t)\} = \mathbf{A}_1 \mathbf{R}_s \mathbf{A}_1^H + \sigma_n^2 \mathbf{I}_N \quad (14)$$

If  $\hat{\mathbf{A}}_1$  is a matrix with full column rank (i.e.,  $N > K + 1$ ), then  $\hat{\mathbf{A}}_1^+ \hat{\mathbf{A}}_1 \approx \mathbf{I}_K$ , and  $\hat{\mathbf{R}}_s$  can be expressed as

$$\begin{aligned}\hat{\mathbf{R}}_s &= (\hat{\mathbf{A}}_1^+ \hat{\mathbf{A}}_1^H) \mathbf{R}_s \left( \hat{\mathbf{A}}_1^H (\hat{\mathbf{A}}_1^H)^+ \right) + \sigma_n^2 (\hat{\mathbf{A}}_1^+ \hat{\mathbf{A}}_1^H) \mathbf{I}_K \left( \hat{\mathbf{A}}_1^H (\hat{\mathbf{A}}_1^H)^+ \right) \\ &\approx \mathbf{R}_s + \sigma_n^2 \mathbf{I}_K\end{aligned}\quad (15)$$

Similarly, the estimate value  $\bar{\mathbf{s}}(t)$  of  $\mathbf{s}(t)$  can be derived from the received signal  $\mathbf{x}_2(t)$  of subarray 2 as follows

$$\bar{\mathbf{s}}(t) = (\hat{\mathbf{A}}_2^H \hat{\mathbf{A}}_2)^{-1} \hat{\mathbf{A}}_2^H \mathbf{x}_2(t) = \hat{\mathbf{A}}_2^+ \mathbf{x}_2(t) \quad (16)$$

If  $\{\hat{\alpha}_k\}_1^K$  and  $\{\hat{\beta}_k\}_1^K$  match,  $\bar{\mathbf{R}}_s$  can be obtained as follows

$$\bar{\mathbf{R}}_s = E \{ \bar{\mathbf{s}}(t) \bar{\mathbf{s}}^H(t) \} = \hat{\mathbf{A}}_2^+ \mathbf{R}_{21} \left( \hat{\mathbf{A}}_1^H \right)^+ \quad (17)$$

where  $\mathbf{R}_{21} = E \{ \mathbf{x}_2(t) \mathbf{x}_1^H(t) \}$  is the cross-covariance matrix.

Define a  $K \times K$  dimensional permutation matrix  $\mathbf{T}$ , which satisfies  $\forall \mathbf{T}_{pq} \in \{0, 1\}$ ,  $\sum_1^K \mathbf{T}_{pq} = 1$ , and  $\sum_1^K \mathbf{T}_{qp} = 1$ . Sorting  $\{\hat{\alpha}_k\}_1^K$  by  $\mathbf{T}$ , the array manifold matrix of subarray 2 satisfies  $\hat{\mathbf{A}}_2 \mathbf{T} = \mathbf{A}_2$  and  $\hat{\mathbf{A}}_2^+ \approx \mathbf{T} \hat{\mathbf{A}}_2^+$ . Accordingly, (17) can be transformed into

$$\bar{\mathbf{R}}_s \approx \mathbf{T} \hat{\mathbf{A}}_2^+ \left( \hat{\mathbf{A}}_2 \mathbf{R}_s \hat{\mathbf{A}}_1^H \right) \left( \hat{\mathbf{A}}_1^H \right)^+ \approx \mathbf{T} \hat{\mathbf{R}}_s \quad (18)$$

If the received signal is incoherent and  $\bar{\mathbf{R}}_s$  is invertible,  $\mathbf{T} = \bar{\mathbf{R}}_s \bar{\mathbf{R}}_s^{-1}$ , then  $\mathbf{T} \{\hat{\alpha}_k\}_1^K$  and  $\{\hat{\beta}_k\}_1^K$  are matching pair.

If the received signal is coherent and  $\bar{\mathbf{R}}_s$  is a singular matrix,  $\mathbf{T}$  can be solved by the function as follows

$$\mathbf{J}_{\text{PSCM}} = \min_{\mathbf{T}} \|\bar{\mathbf{R}}_s - \mathbf{T} \hat{\mathbf{R}}_s\|_F \quad (19)$$

To reduce computational complexity, the following cost function can be formulated

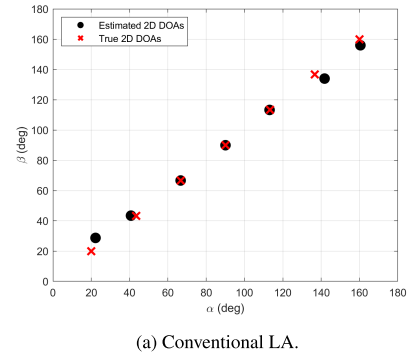
$$\mathbf{J}_{\text{PSCM}} = \min_{\mathbf{T}_n} \|\bar{\mathbf{R}}_{sm} - \mathbf{T}_n \hat{\mathbf{R}}_s\|_F \quad (20)$$

where  $\mathbf{T}_n$  denotes the  $n$ -th row of  $\mathbf{T}$ , and  $\bar{\mathbf{R}}_{sm}$  denotes the  $m$ -th row of  $\bar{\mathbf{R}}_s$ . Then the correspondence between  $\{\hat{\alpha}_k\}_1^K$  and  $\{\hat{\beta}_k\}_1^K$  can be obtained from  $\mathbf{T}$ .

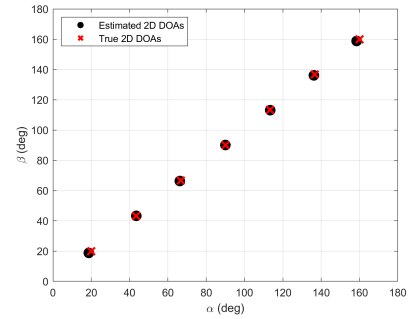
#### 4. Numerical simulations

The first simulation compares the DOA resolution capabilities of different LAs with 15 elements. The signal-to-noise ratio (SNR) is set to 0 dB, and the number of snapshots is fixed at  $J = 200$ . Seven sources are uniformly distributed in the range of  $20^\circ$  to  $160^\circ$ . The mutual coupling model is characterized by coupling coefficients  $c_1 = 0.3e^{j\pi/3}$ ,  $B = 100$ , and  $c_\ell = c_1 e^{-j(\ell-1)\pi/8}/\ell$  for  $2 \leq \ell \leq B$ .

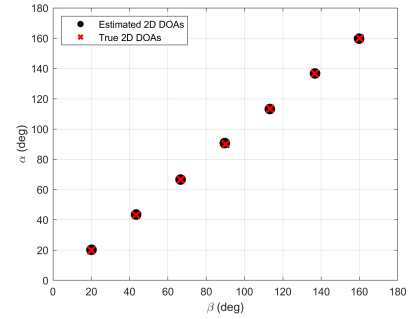
Figure 3 depicted the 2-D DOA estimates scatter plots of conventional LA and improved nested LAs in the presence of mutual coupling. The red crosses indicate estimated results, and black circles indicate actual values. The conventional LA fails to identify all sources due to its ULA-based subarray configuration with limited DOFs and strong mutual coupling, which degrades its 2-D DOA estimation accuracy. In contrast, ISNA-LA achieves superior performance using the 2-D MUSIC algorithm, yielding estimated DOAs that closely match the true DOAs. ANCADI-S-LA and AINA-LA achieve complete source resolution through optimized subarray designs, which offer higher DOFs, larger apertures, and reduced mutual coupling compared to the conventional LA and ISNA-LA. The LASSO-PSCM algorithm further enhances estimate performance by fully utilizing the achieved



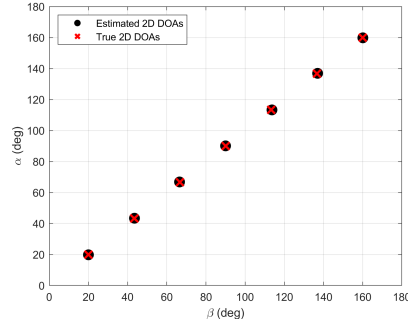
(a) Conventional LA.



(b) ISNA-LA.



(c) ANCADI-S-LA.



(d) AINA-LA.

**Fig. 3** DOAs scatter plots of conventional LA and improved nested LAs in the presence of mutual coupling.

DOFs and ensuring accurate DOA angles pairing.

The root mean square error (RMSE) of DOA estimates is evaluated via 200 Monte Carlo trials, with three sources located at  $(\alpha_1, \beta_1) = (20^\circ, 20^\circ)$ ,  $(\alpha_2, \beta_2) = (40^\circ, 40^\circ)$  and  $(\alpha_3, \beta_3) = (60^\circ, 60^\circ)$ . Figure 4 illustrates the RMSE of the DOA estimates versus the SNR with  $J = 200$ . The RMSE of all LAs decreases with increasing SNR and stabilizes beyond 12.5 dB. Conventional LA have the highest RMSE across the SNR range since it has strong mutual coupling and limited DOFs. The RMSE of TLNA-LA is slightly lower than that

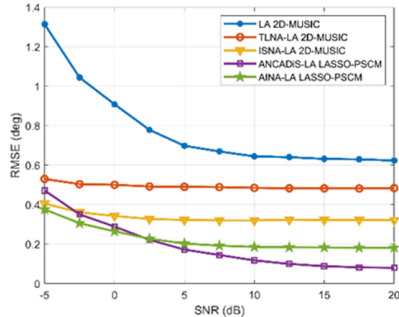


Fig. 4 RMSE DOA estimates versus the SNR with  $J = 200$  in the presence of mutual coupling.

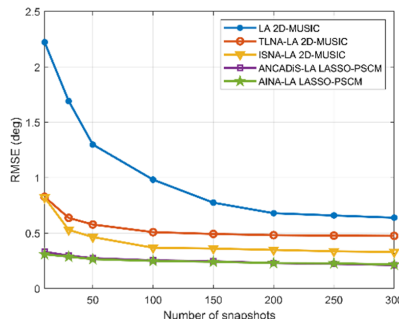


Fig. 5 RMSE of DOA estimates versus the number of snapshots with SNR = 0 dB in the presence of mutual coupling.

of LA, which is due to the fact that the mutual coupling effect between its elements is lower than that of LA. ISNA-LA shows intermediate performance, with reduced mutual coupling compared to conventional LA though equivalent DOFs to TLNA-LA. When SNR is below 2.5 dB, AINA-LA has lower RMSE than ANCADI-S-LA due to its sparser element distribution, which reduces mutual coupling that dominate DOA estimation performance in low-SNR conditions. Conversely, at SNRs above 5 dB, ANCADI-S-LA outperforms AINA-LA due to its larger array aperture, emphasizing the importance of aperture size in high-SNR regimes.

Figure 5 shows the RMSE of the DOA estimates versus the number of snapshots with SNR = 0 dB. The RMSE decreases with more snapshots and stabilizes beyond 100 snapshots. Conventional LA exhibits the highest RMSE due to limited DOFs and strong mutual coupling in its ULA subarrays. ISNA-LA outperforms TLNA-LA, achieving lower RMSE by reducing mutual coupling through its IOTLNA subarray. ANCADI-S-LA and AINA-LA demonstrate the lowest and nearly identical RMSE curves, thanks to their advanced subarrays (ANCADI-S and AINA), which maximize DOFs while minimizing mutual coupling. This highlights the critical role of subarray design in balancing DOFs and coupling suppression for accurate DOA estimation.

## 5. Conclusions

This paper presents three improved nested LAs (ISNA-LA, AN-CADI-S-LA, AINA-LA) that effectively address the fundamental trade-off between DOFs and mutual coupling in 2-D DOA estimation. By systematically optimizing the sparse arrangement of orthogonal subarrays, these configurations

achieve enhanced DOFs and reduced mutual coupling effect. A novel LASSO-PSCM algorithm is developed to fully exploit virtual array in difference coarray domain, enabling computationally efficient 2-D parameter estimation with automatic angles pairing. Simulation results validate the superiority of the proposed LA configurations and LASSO-PSCM method in enhancing DOA estimation performance.

## Acknowledgments

This work was jointly supported in part by the National Natural Science Foundation of China under Grant Nos. 62373262, 62303336, and 62403336, in part by the Guangxi Key Laboratory of Brain-inspired Computing and Intelligent Chips under Grant No. BCIC-24-K9, and in part by the Guidance Project of Science and Technology Research Plan of Hubei Provincial Department of Education under Grant No. B2017477.

## References

- [1] P. Pal and P.P. Vaidyanathan, “Nested arrays: A novel approach to array processing with enhanced degrees of freedom,” *IEEE Trans. Signal Process.*, vol. 58, no. 8, pp. 4167–4181, Aug. 2020. DOI: [10.1109/tsp.2010.2049264](https://doi.org/10.1109/tsp.2010.2049264)
- [2] Y. Hua, T.K. Sarkar, and D.D. Weiner, “An L-shaped array for estimating 2-D directions of wave arrival,” *IEEE Trans. Antennas Propag.*, vol. 39, no. 2, pp. 143–146, Feb. 1991. DOI: [10.1109/8.68174](https://doi.org/10.1109/8.68174)
- [3] X. Li, X. Wang, W. Wang, and S. Ren, “Generalized L-shaped array based on the difference and sum coarray concept,” *IEEE Access*, vol. 8, pp. 140456–140466, June 2020. DOI: [10.1109/ACCESS.2020.3012527](https://doi.org/10.1109/ACCESS.2020.3012527)
- [4] W. Yu, P. He, F. Pan, A. Cui, and Z. Xu, “Improved optimal configuration for reducing mutual coupling in a two-level nested array with an even number of sensors,” *IEICE Trans. Commun.*, vol. E105-B, no. 7, pp. 856–865, July 2022. DOI: [10.1587/transcom.2021EBP3131](https://doi.org/10.1587/transcom.2021EBP3131)
- [5] W. Yu, P. He, F. Pan, D. Qiu, A. Fang, and Z. Xu, “Augmented nested coprime array with displaced subarrays design achieving reduced mutual coupling,” *Int. J. Electron.*, vol. 110, no. 4, pp. 734–752, April 2023. DOI: [10.1080/00207217.2022.2062794](https://doi.org/10.1080/00207217.2022.2062794)
- [6] W. Yu, P. He, H. Liu, and D. Qiu, “Augmented improved nested array with enhanced degrees of freedom and reduced mutual coupling effect,” *Electron. Lett.*, vol. 59, no. 21, e13002, Nov. 2023. DOI: [10.1049/el12.13002](https://doi.org/10.1049/el12.13002)